Calculation of Coster–Kronig Enhancement Factors of the Some Elements in the Atomic Number Range $50 \leq Z \leq 59$

R. Yilmaz*

Department of Physics, Faculty of Sciences, Yüzüncü Yil University, 65080 Van, Turkey

(Received January 24, 2014; in final form June 8, 2016)

L X-ray fluorescence cross-sections of some elements in the atomic number range $50 \leq Z \leq 59$ have been calculated theoretically according to subshell excitation energies of elements. The Coster–Kronig transitions (f_{12}, f_{23}, and f_{13}) are non-radiative transitions. The Coster–Kronig enhancement factors due to the effect of the Coster–Kronig transitions on L X-ray fluorescence cross-sections have been calculated theoretically. The calculated values have been compared with other earlier experimental and theoretical values.

DOI: 10.12693/APhysPolA.130.1269

PACS/topics: 32.30.Rj, 32.50. +d, 32.30.–r

1. Introduction

X-ray fluorescence (XRF) cross-sections are required for many practical applications, like elemental analysis by X-ray emissions technique, basic studies of nuclear and atomic processes leading to emission of X-rays and Auger electrons and dosimetric computations for medical physics and irradiational processes. The accuracy and reliability of the results depend on the calculated and tabulated values of such cross-sections.

A survey of the literature shows that the L shell XRF cross-sections have been well explored both experimentally and theoretically over the whole range of elements in the periodic table. The experimental and theoretical data for subshell fluorescence yields, the Coster–Kronig transitions probability and Auger yields of the L shell are also available for a large number of elements.

The XRF cross-section is defined as the product of corresponding photoelectric cross-section and fluorescence yield at a given excitation energy. However, in the case of the L shell, particularly the L_3 subshell X-ray lines, estimation of XRF cross-sections is not so straight forward because of the possibility of the so-called Coster–Kronig transitions. These transitions are non-radiative transitions in which the two inner shells electrons are situated on two different subshells of the same inner shell (e.g. L_1 and L_3). Such transitions between L_1 andL_3 and between L_2 and L_3 sublevels cause an additional excitation of L_3 subshell state, thereby enhancing the fluorescence cross-sections for L_α and other subshell X-ray lines [1, 2].

Recently, many researchers have investigated fluorescence cross-sections, the Coster–Kronig transitions, fluorescence yields for various elements [3–11]. Chemical effects on the K_β/K_α intensity ratios and on the enhancement of the Coster–Kronig transitions have been investigated [12, 13]. The effect of the Coster–Kronig yields on L X-ray emission cross-sections has been studied [14]. Theoretical and experimental Coster–Kronig enhancement factors of the some elements in atomic number range $66 \leq Z \leq 72$ and $74 \leq Z \leq 90$ have been investigated [15, 16]. In a previous work, we investigated theoretical and experimental Coster–Kronig enhancement factors for Yb, Lu, Os, Pt elements [17].

In the present study, we studied the role of the Coster–Kronig transitions on L XRF cross-sections. To investigate the effect of the Coster–Kronig transitions on L XRF cross-sections, excitation energies were chosen according to binding energies for each element and calculated XRF cross-sections. Then, theoretical Coster–Kroning enhancement factors have been calculated. The excitation energies have been chosen such that $B_{L2} < E < B_{L1}$ and $B_{L1} < E < B_K$, where the L_1 and L_2 are the subshells, B_L's are the binding energies of the subshells, K is the ground shell and E is the excitation energy.

2. Theoretical L XRF cross-sections and calculation of Coster–Kronig enhancement factors

The values of the L XRF cross-sections have been calculated from the theoretical L_i subshell photoionization cross-sections [18], and radiative decay rates [19, 20], semi-empirically fitted values of fluorescence yields and Coster–Kronig transition probabilities, using the following equations [6]:

$$\sigma_{L\ell} = [\sigma_1(f_{13} + f_{12}f_{23}) + \sigma_2 f_{23} + \sigma_3]\omega_3 F_{3l}, \quad (1)$$

$$\sigma_{L\alpha} = [\sigma_1(f_{13} + f_{12}f_{23}) + \sigma_2 f_{23} + \sigma_3]\omega_3 F_{3\alpha}, \quad (2)$$

$$\sigma_{L\beta} = \sigma_1\omega_1 F_{1\beta} + (\sigma_1 f_{12} + \sigma_2)\omega_2 F_{2\beta} + [\sigma_3 + \sigma_2 f_{23} + \sigma_1(f_{13} + f_{12}f_{23})]\omega_3 F_{3\beta}, \quad (3)$$

where σ_1, σ_2 and σ_3 are the L subshell photoionization cross-sections interpolated from the tables of Scofield [18], at the selected excitation energies. ω_1, ω_2 and ω_3 are fluorescence yield for the L_1, L_2, L_3 subshell. f_{12}, f_{13} and f_{23} are the Coster–Kronig transition probabilities. In these calculations, fluorescence yield and

*e-mail: ryilmaz@yyu.edu.tr

TABLE I

Theoretical L subshell fractions of the radiative widths calculated.

Element	Fraction of radiative widths				
	$F_{3\ell}$	$F_{3\alpha}$	$F_{1\beta}$	$F_{2\beta}$	$F_{3\beta}$
^{50}Sn	0.031	0.858	0.827	0.864	0.109
^{51}Sb	0.031	0.851	0.820	0.860	0.115
^{52}Te	0.031	0.847	0.812	0.853	0.120
^{53}I	0.031	0.841	0.805	0.848	0.125
^{54}Xe	0.032	0.837	0.798	0.843	0.130
^{56}Ba	0.032	0.828	0.786	0.835	0.139
^{59}Pr	0.032	0.823	0.781	0.830	0.143

the Coster–Kronig transition probabilities are taken from table of Krause [21]. F_{ij} $(F_{3\alpha}, F_{3\ell}, F_{3\beta}, F_{2\beta}, F_{1\beta})$ are the fractions of the radiation width of the subshells L_i (L_1, L_2, L_3) contained in the j-th spectral line, i.e. calculated F_{ij} values are presented in Table I:

$$F_{ij} = \frac{\Gamma_{ij}}{\Gamma} \quad \text{e.g.} \quad F_{3\ell} = \frac{\Gamma_{3\ell}}{\Gamma}, \tag{4}$$

where Γ is the theoretical total radiative transition rate of the L_3 shell and $\Gamma_{3\alpha}$ is the sum of the radiative transition rates contributing to the L_α lines associated with the hole filling in the L_3 shell. That is

$$\Gamma_{3\ell} = \Gamma_3(M_1 - L_3), \tag{5}$$

$$\Gamma_{3\alpha} = \Gamma_3(M_4 - L_3) + \Gamma_3(M_5 - L_3), \tag{6}$$

$$\Gamma_{3\beta} = \Gamma_3(N_1 - L_3) + \Gamma_3(N_4 - L_3) + \Gamma_4(N_5 - L_3) + \Gamma_3(O_1 - L_3) + \Gamma_3(O_4, O_5 - L_3), \tag{7}$$

$$\Gamma_{2\beta} = \Gamma_2(M_4 - L_2) + \Gamma_2(M_3 - L_2), \tag{8}$$

$$\Gamma_{1\beta} = \Gamma_1(M_2, M_3 - L_1) + \Gamma_1(M_4, M_5 - L_1), \tag{9}$$

where $\Gamma_{3\ell}$, $\Gamma_{3\alpha}$, $\Gamma_{3\beta}$ are the radiative transition rates from the $(M_1,\ M_4,\ M_5)$, $(N_1,\ N_4,\ N_5)$, $(O_1,\ O_4,\ O_5)$ to the L_3. $\Gamma_{2\beta}$ is the radiative transition rates from the $(M_4,\ M_3)$ to the L_2 shell and $\Gamma_{1\beta}$ is the radiative transition rates from the $(M_2,\ M_3,\ M_4,\ M_5)$ to the L_1. Radiative transition rates were calculated by Scofield using Hartree–Slater theory for many elements [19, 20]. As mentioned before, it is known that the Coster–Kronig transitions are non-radiative transitions. If the Coster–Kronig transitions do not exist ($f_i = 0$), L XRF cross-sections can be calculated using the following equations [15]:

$$\sigma_{L\ell} = \sigma_3\omega_3 F_{3l}, \tag{10}$$

$$\sigma_{L\alpha} = \sigma_3\omega_3 F_{3\alpha}, \tag{11}$$

$$\sigma_{L\beta} = \sigma_1\omega_1 F_{1\beta} + \sigma_2\omega_2 F_{2\beta} + \sigma_3\omega_3 F_{3\beta}. \tag{12}$$

In fact, Coster–Kronig transitions are present. In this situation, L XRF were evaluated using Eqs. (1)–(3). The Coster–Kronig enhancement factors $\kappa_{ij} (i = \ell, \alpha, \beta;\ j = 1, 2)$ can be calculated using the relations [15, 16]:

$$\kappa_{l,\alpha} = \frac{\sigma_1(f_{13} + f_{12}f_{23}) + \sigma_2 f_{23} + \sigma_3}{\sigma_3}, \tag{13}$$

$$\kappa_\beta = [\sigma_1\omega_1 F_{1\beta} + (\sigma_1 f_{12} + \sigma_2)\omega_2 F_{2\beta} + [\sigma_3 + \sigma_2 f_{23} + \sigma_1(f_{13} + f_{12}f_{23})]\omega_3 F_{3\beta}]/ [\sigma_1\omega_1 F_{1\beta} + \sigma_2\omega_2 F_{2\beta} + \sigma_3\omega_3 F_{3\beta}]. \tag{14}$$

In this calculations, when L_3 and L_2 were excited, the Coster–Kronig enhancement factors were represented by κ_{i1}; when L_3, L_2 and L_1 were excited, Coster–Kronig enhancement factors were represented by κ_{i2}.

3. Results and discussion

The L subshell XRF cross-sections have been calculated using Eqs. (1)–(3) for some elements in the atomic number range $50 \leq Z \leq 59$ and are given in Tables II–IV. The values of the Coster–Kronig enhancement factors for same elements have been determined theoretically using Eqs. (13), (14), and are listed in Tables V, VI.

TABLE II

L_3 XRF cross-sections (barns/atom) for $50 \leq Z \leq 59$.

Element	E [keV]	$\sigma_{L\alpha}$	$\sigma_{L\beta}$	σ_{Ll}
		Calculated	Calculated	Calculated
^{50}Sn	4.190	6114.673	4051.507	228.052
	5.000	3873.648	3434.045	144.471
^{51}Sb	4.417	6106.195	4068.398	237.063
	5.000	4460.459	3845.085	173.169
^{52}Te	4.651	6068.833	4116.672	224.298
	5.000	5098.527	4343.044	203.866
^{53}I	4.892	6061.518	4164.999	230.639
	5.199	5195.983	4515.587	197.675
^{54}Xe	5.140	6084.278	4182.044	232.611
	5.455	5235.263	4786.046	200.153
^{56}Ba	5.670	6055.576	4356.180	233.394
	6.000	5233.892	4670.859	201.643
^{59}Pr	6.488	6178.926	4554.502	240.249
	6.848	5180.996	4848.077	205.618

TABLE III

L_2 XRF cross-sections (barns/atom) for $50 \leq Z \leq 59$.

Element	E [keV]	$\sigma_{L\alpha}$	$\sigma_{L\beta}$	σ_{Ll}
		Calculated	Calculated	Calculated
^{50}Sn	4.190	6616.083	4108.229	246.753
^{51}Sb	4.417	6606.904	4125.356	256.503
^{52}Te	4.651	6560.409	4186.656	242.467
^{53}I	4.892	6564.625	4239.969	249.783
^{54}Xe	5.140	6601.442	4257.321	252.384
^{56}Ba	5.670	6564.245	4438.948	253.000
^{59}Pr	6.488	6710.314	4645.592	260.911

We calculated that the presence of nonradiative transitions cause changes in the X-ray intensities. It is known that the nonradiative transitions compete with radiative transitions, and they together determine both the absolute and the relative intensities of generated X-rays [11].

TABLE IV

L_1 XRF cross-sections (barns/atom) for $50 \leq Z \leq 59$.

Element	E [keV]	$\sigma_{L\alpha}$	$\sigma_{L\beta}$	σ_{Ll}
		Calculated	Calculated	Calculated
^{50}Sn	5.000	4601.894	3753.412	171.632
^{51}Sb	5.000	5285.625	4233.439	205.206
^{52}Te	5.000	6021.361	4807.750	220.380
^{53}I	5.199	6152.044	4985.208	234.048
^{54}Xe	5.455	6209.023	5293.367	237.382
^{56}Ba	6.000	6202.163	5156.629	238.948
^{59}Pr	6.848	6212.015	5357.	246.536

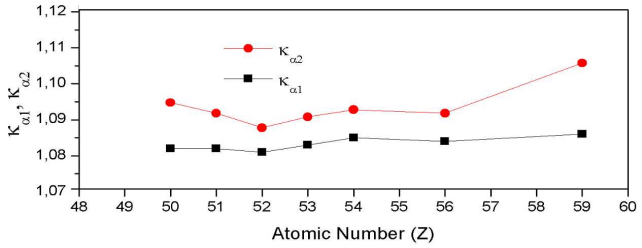

Fig. 1. $\kappa_{\alpha 1}$, $\kappa_{\alpha 2}$ versus atomic number.

The values of the Coster–Kronig enhancement factors (for $\kappa_{\alpha 1}$, $\kappa_{\alpha 2}$ and $\kappa_{\beta 1}$, $\kappa_{\beta 2}$) versus atomic number have been shown in Figs. 1, 2. In the present work, the results indicate up to 8.6% for theoretical value $\kappa_{\alpha 1}$ and 19.9% for theoretical $\kappa_{\alpha 2}$ enhancements of the XRF cross-sections; up to 8.6% for theoretical value of $\kappa_{\ell 1}$ and up to 19.9% for theoretical value $\kappa_{\ell 2}$ enhancements of the XRF cross-sections; up to 2% for theoretical $\kappa_{\beta 1}$ and up to 10.5% for theoretical $\kappa_{\beta 2}$.

Enhancements up to 65% in the XRF cross-sections have been reported by Rani et al. [2] and they also reported 24% the measurement of $\kappa_{\alpha 2}$ Coster–Kronig enhancement factor for ^{51} Sb. Theoretical predictions are up to 21% as seen in Table V. Good agreement is observed between present studies and the studies done by Rani et al. for $\kappa_{\alpha 2}$.

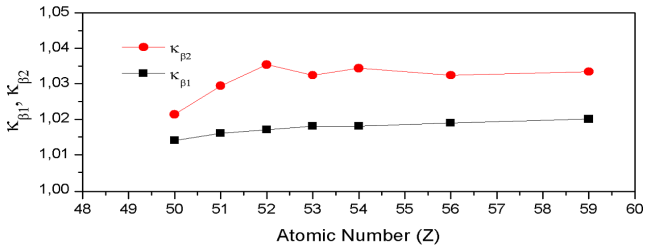

Fig. 2. $\kappa_{\beta 1}$, $\kappa_{\beta 2}$ versus atomic number.

The measurements of the Coster–Kronig enhancement factors of some elements in the atomic number range $66 \leq Z \leq 72$ and $74 \leq Z \leq 90$ using photoionization method have been investigated [15, 16]. Öz et al. reported the theoretical $\kappa_{\alpha 1}$, $\kappa_{\ell 1}$ Coster–Kronig enhancement factors as 8–9% and up to 4–6% for experimental; up to 20–30% for theoretical $\kappa_{\alpha 2}$, $\kappa_{\ell 2}$ and up to 14–24% for experimental. In addition, the theoretical $\kappa_{\beta 1}$ Coster–Kronig enhancement factors have been reported by Öz et al., as 2%, 9–11% for $\kappa_{\beta 2}$ and up to 1–2% for experimental $\kappa_{\beta 1}$, 8–11% for $\kappa_{\beta 2}$.

TABLE V

$\kappa_{l1}-\kappa_{\alpha 1}$ and $\kappa_{l2}-\kappa_{\alpha 2}$ Coster–Kronig enhancement factors for $50 \leq Z \leq 59$.

Element	E [keV]	$\kappa_{l1}, \kappa_{\alpha 1}$	E [keV]	$\kappa_{l2}, \kappa_{\alpha 2}$	Rani et al. (for $\kappa_{\alpha 2}$)	Rani et al. (for $\kappa_{\alpha 2}$)
	(for L_2)	Calculated	(for L_1)	Calculated	Measured	Calculated (for 22.6 keV)
^{50}Sn	4.190	1.082	5.000	1.188	–	1.190
^{51}Sb	4.417	1.082	5.000	1.185	1.24 ± 0.05	1.210
^{52}Te	4.651	1.081	5.000	1.181	–	1.200
^{53}I	4.892	1.083	5.199	1.184	–	–
^{54}Xe	5.140	1.085	5.455	1.186	–	1.140
^{56}Ba	5.670	1.084	6.000	1.185	–	1.200
^{59}Pr	6.488	1.086	6.848	1.199	–	–

From L shell studies, one can see, due to the Coster–Kronig transitions, there is an enhancement up to 2–20% for theoretical; up to 1–24% for experimental each element. Also, this has been observed in our earlier both theoretical and experimental studies [17]. Thus, it must be taken into account in quantitative XRF cross-sections.

TABLE VI

$\kappa_{\beta 1}$ and $\kappa_{\beta 2}$ Coster–Kronig enhancement factors for $50 \leq Z \leq 59$.

Element	E [keV] (for L_2)	$\kappa_{\beta 1}$ Calculated	E [keV] (for L_1)	$\kappa_{\beta 2}$ Calculated
^{50}Sn	4.190	1.014	5.000	1.093
^{51}Sb	4.417	1.016	5.000	1.101
^{52}Te	4.651	1.017	5.000	1.107
^{53}I	4.892	1.018	5.199	1.104
^{54}Xe	5.140	1.018	5.455	1.106
^{56}Ba	5.670	1.019	6.000	1.104
^{59}Pr	6.488	1.020	6.848	1.105

References

[1] J.L. Labar, *X-ray Spectrom.* **20**, 111 (1991).

[2] A. Rani, N. Nath, S.N. Chaturvedi, *X-ray Spectrom.* **18**, 77 (1989).

[3] M. Ertuğrul, *J. Electron Spectrosc. Relat. Phenom.* **125**, 69 (2002).

[4] M. Ertuğrul, *Appl. Radiat. Isot.* **57**, 63 (2002).

[5] M. Ertuğrul, *J. Quant. Spectrosc. Radiat. Transf.* **72**, 567 (2002).

[6] E. Tiraşoğlu, U. Çevik, B. Ertuğrul, Y. Atalay, A.İ. Kopya, *Radiat. Phys. Chem.* **60**, 11 (2001).

[7] I. Han, L. Demir, M. Ağbaba, *Radiat. Phys. Chem.* **76**, 1551 (2007).

[8] A. Kaya, M. Ertuğrul, O. Doğan, Ö. Söğüt, Ü. Turgut, Ö. Şimşek, *Anal. Chem. Acta* **441**, 317 (2001).

[9] E. Öz, Y. Özdemir, N. Ekinci, M. Ertuğrul, Y. Şahin, H. Erdoğan, *Spectrochim. Acta B* **55**, 1869 (2000).

[10] E. Öz, N. Ekinci, Y. Özdemir, M. Ertuğrul, Y. Şahin, H. Erdoğan, *J. Phys. B At. Mol. Opt. Phys.* **34**, 631 (2001).

[11] S. Puri, N. Singh, *Radiat. Phys. Chem.* **75**, 2232 (2006).

[12] A. Küçükönder, E. Büyükkasap, R. Yılmaz, Y. Şahin, *Acta Phys. Pol. A* **95**, 243 (1999).

[13] Ö. Söğüt, E. Büyükkasap, M. Ertuğrul, A. Küçükönder, *J. Quant. Spectrosc. Radiat. Transf.* **74**, 395 (2002).

[14] A.B. Hallak, *Radiat. Phys. Chem.* **60**, 17 (2001).

[15] E. Öz, N. Ekinci, M. Ertuğrul, Y. Şahin, *X-ray Spectrom.* **32**, 153 (2003).

[16] E. Öz, Y. Sahin, M. Ertuğrul, *Radiat. Phys. Chem.* **69**, 17 (2004).

[17] R. Yılmaz, E. Öz, M. Tan, R. Durak, A.İ. Demirel, Y. Şahin, *Radiat. Phys. Chem.* **78**, 318 (2009).

[18] J.H. Scofield, *Report UCRL, No. 51326*, Lawrence Livermore Laboratory Report, California 1973.

[19] J.H. Scofield, *Phys. Rev. A* **179**, 9 (1969).

[20] J.H. Scofield, *At. Data Nucl. Data Tables* **14**, 121 (1974).

[21] M.O. Krause, *J. Phys. Chem. Ref. Data* **8**, 307 (1979).